PAR3-aPKC regulates Tiam1 by modulating suppressive internal interactions

Kenji Matsuzawa[a], Hiroki Akita[a], Takashi Watanabe[a,†], Mai Kakeno[a], Toshinori Matsui[a], Shujie Wang[b], and Kozo Kaibuchi[a,*]

[a]Department of Cell Pharmacology, Nagoya University Graduate School of Medicine, Nagoya 466-8550, Japan; [b]Department of Neural Regeneration and Cell Communication, Graduate School of Medicine, Mie University, Tsu 514-8507, Japan

ABSTRACT Tiam1 is one of the most extensively analyzed activators of the small GTPase Rac. However, fundamental aspects of its regulation are poorly understood. Here we demonstrate that Tiam1 is functionally suppressed by internal interactions and that the PAR complex participates in its full activation. The N-terminal region of Tiam1 binds to the protein-binding and catalytic domains to inhibit its localization and activation. Atypical PKCs phosphorylate Tiam1 to relieve its intramolecular interactions, and the subsequent stabilization of its interaction with PAR3 allows it to exert localized activity. By analyzing Tiam1 regulation by PAR3-aPKC within the context of PDGF signaling, we also show that PAR3 directly binds PDGF receptor β. Thus we provide the first evidence for the negative regulation of Tiam1 by internal interactions, elucidate the nature of Tiam1 regulation by the PAR complex, and reveal a novel role for the PAR complex in PDGF signaling.

INTRODUCTION

T-cell lymphoma invasion and metastasis 1 (Tiam) was first identified as a proinvasion factor in T-lymphocytes (Habets et al., 1994) and is now widely recognized as a critical regulator of various cellular functions during development and disease in multiple cell types (reviewed in Mertens et al., 2003; Cook et al., 2014). A typical member of the Dbl family of guanine nucleotide exchange factors (GEFs), that is, activators for the Rho small GTPases, its functional core is a carboxyl (C)-terminal tandem Dbl homology/pleckstrin homology (DHPH) domain. It exhibits exchange activity only for Rac1 in vivo (Michiels et al., 1995). Protein–protein interactions play an important

role in localizing Tiam1 to specific membrane subdomains (Bourguignon et al., 2000; Nishimura et al., 2005; Tolias et al., 2005, 2007; Miyamoto et al., 2006). These interactions are primarily mediated through a modified PH domain near the amino (N)-terminal region, the coiled-coil/extended region (PHnCCEx) domain (Stam et al., 1997; Terawaki et al., 2010).

One of the most extensively characterized interactions is the direct binding of Tiam1 with partitioning defective 3 (PAR3), through which Tiam1 forms a complex with other PAR polarity proteins, namely PAR6 and atypical protein kinase C (aPKC; PAR complex; Nishimura et al., 2005). The PAR complex is a crucial, intrinsic determinant of cell polarity (Suzuki and Ohno, 2006). The functional interaction between Tiam1 and PAR3 is required for many cell polarization events, including axon specification (Nishimura et al. 2005), dendritic spine morphogenesis (Zhang and Macara, 2006), and synaptogenesis (Duman et al., 2013) in neurons, as well as for both chemotactic (Pegtel et al., 2007) and haptotactic (Wang et al., 2012) directional cell migration. The interaction of Tiam1 with PAR3 serves to spatially restrict Rac1 activation and localize cytoskeletal remodeling (reviewed in Iden and Collard, 2008). An additional functional interaction with the PAR complex exists through aPKC, as aPKC activity is required for proper signaling through Tiam1 during polarized migration (Pegtel et al., 2007; Wang et al., 2012). Moreover, Tiam1 is an aPKC substrate in vitro, with the phosphorylation site(s) residing within the N-terminal inhibitory region (Wang et al., 2012).

These observations suggest a crucial role for Tiam1 phosphorylation by aPKC. Because many of the basic aspects of Tiam1 regulation remain poorly understood, we performed a detailed analysis regarding the function of Tiam1 phosphorylation by aPKC. We show that Tiam1 is regulated by internal interactions in a signal-sensitive manner that is dependent on its phosphorylation by aPKC. Incidental to this demonstration, our work also expands the role of the PAR complex in receptor tyrosine kinase (RTK) signaling by identifying PAR3 as a novel interacting partner for platelet-derived growth factor (PDGF) receptor β (PDGFRβ) and by revealing its role in mediating PDGF signaling to Rac1 through Tiam1.

RESULTS

Phosphorylation of Tiam1 by aPKC
We previously identified Tiam1 as a novel substrate of aPKC in vitro and mapped the phosphorylation site(s) to the N-terminal region (Tiam1-N392; Wang et al., 2012). As an initial step toward identifying potential phosphorylation site(s), we performed in vitro phosphorylation assays on the N-terminal Tiam1 fragments Tiam1-N/1 (amino acids [aa] 1–130), Tiam1-N/2 (aa 131–260) and Tiam1-N/3 (aa 261–392) using the catalytic domain of aPKCλ (aPKCλ-cat). Tiam1-N/1 was phosphorylated at least as efficiently as the full-length N-terminal fragment, whereas neither Tiam1-N/2 nor Tiam1-N/3 was phosphorylated (Figure 1, A and B). We also found that the N-terminal-most 50 amino acids (–N50) were phosphorylated with a stoichiometry similar to that of the longer fragments (unpublished data). On the basis of these results, we next determined the specific residues that were phosphorylated by examining the in vitro phosphorylation of Tiam1-N/1, in which the serine and threonine residues of the consensus PKC phosphorylation motifs ([S/T]-X-[R/K], [R/K]-X-[S/T], and [R/K]-X-X-[S/T]) within the most N-terminal 50 aa were mutated to alanine. The Ser-29 (A29) and Ser-33 (A33) mutations resulted in significant reductions in phosphorylation, to as much as 40% that of the wild-type (WT) fragment when both residues were simultaneously mutated, suggesting that these two serine residues are primarily phosphorylated by aPKC in vitro (Figure 1C). Tiam2/STEF is a Tiam1 homologue, with a similar overall domain architecture (Chiu et al., 1999). We found that the analogous N-terminal region of Tiam2/STEF (N463) was also phosphorylated by aPKC in vitro (Supplemental Figure S1B).

To analyze the significance of these phosphorylation sites, we produced antibodies based on phosphorylation at the respective residues and successfully characterized an anti–phospho-Ser-29 (Tiam1-pS29) antibody (Figure 1, D and E). When this antibody was used in an immunoblot analysis of recombinant N-terminal Tiam1 incubated with aPKCλ-cat in either the absence or presence of ATP, anti-Tiam1-pS29 antibody immunoreactivity was dose dependent and restricted to the proteins that were incubated in the presence of ATP (Figure 1D). Immunoblot analysis of COS-7 cell lysates containing full-length (FL) Tiam (Tiam1-FL–hemagglutinin [HA]) and aPKCλ (myc-aPKCλ) demonstrated that coexpression of aPKCλ-WT enhanced the immunoreactivity of the anti-Tiam1-pS29 antibody, whereas coexpression of kinase-negative (KN) aPKCλ (aPKCλ-KN) reduced this immunoreactivity. Of importance, Tiam1-A29 was not detected even when aPKCλ-WT was coexpressed, suggesting that this antibody is specific for phosphorylation at Ser-29 (Figure 1E).

aPKC phosphorylation regulates Tiam1 interdomain binding
Many modular signaling proteins, including several RhoGEFs, are regulated by interactions among their domains (reviewed in Rossman et al., 2005). The Tiam1 N-terminal region contains no functional domains; however, the region immediately surrounding the

aPKC-phosphorylation sites is highly conserved across species and enriched in basic amino acids (Supplemental Figure S1A). Furthermore, this region is generally considered to be inhibitory, although no mechanistic basis for this assertion has been reported (Michiels et al., 1997; reviewed in Mertens et al., 2003). These observations suggested that the N-terminal region of Tiam1 might mediate intramolecular interaction(s), and its phosphorylation might regulate these interactions by altering the electrochemical properties of this region. Therefore we performed an in vitro binding assay to investigate this possibility; we passed maltose-binding protein (MBP)–fused C-terminal Tiam1 fragments (–PHnCCEx, –RBD/PDZ, and –DHPHc; Figure 1A) through columns of glutathione S-transferase (GST)–Tiam1-N392. The adjacent PHnCCEx domain and, to a lesser extent, the most C-terminal DHPHc region were efficiently pulled down (Figure 2A). A similar binding pattern was observed for Tiam2/STEF (Supplemental Figure S1C). When we analyzed the mode of PHnCCEx binding to the N-terminal region of Tiam1, we found that the intact PHnCCEx fragment was necessary for an efficient interaction (Figure 2B). This result is consistent with a previous structural report that showed that the PHn, CC, and Ex subdomains folded into a single globular domain (Terawaki et al., 2010). In contrast, the DH domain of DHPHc did not contribute significantly to the interaction with the N-terminal region of Tiam1 (Figure 2B). We also characterized the segment of the N-terminal region of Tiam1 that was required for PHnCCEx and DHPHc binding and found that Tiam1-N50, which was the minimum fragment that was phosphorylated by aPKC, was solely responsible for these interactions (Figure 2C). Given this observation, we next investigated whether the aPKC-mediated phosphorylation of the N-terminal region could modulate its interaction with PHnCCEx. Indeed, PHnCCEx binding was severely diminished when Tiam1-N392 was preincubated with aPKC in the presence of ATP. These results indicate that reversible internal interactions mediated by phosphorylation are important factors in Tiam1 regulation (Figure 2E).

Functional significance of Tiam1 intramolecular interactions
The two regions to which the N-terminal region of Tiam1 binds have critical functions: PHnCCEx functions as a protein–protein interaction domain, and the C-terminal PH functions as a regulator of catalytic activity through its interaction with lipid messengers (Baumeister et al., 2003; Viaud et al., 2014). Therefore we investigated the effects of the intramolecular interactions on these functions. When Tiam1 was immunoprecipitated from lysates of NIH-3T3 cells expressing the constitutively active mutant of the two aPKC isoforms, PAR3 coprecipitation was significantly increased compared with the vector control; PAR3 coprecipitation under the WT and KN aPKC conditions was not significantly different from that of the vector control (Figure 3, A and B). To validate that this effect was specifically dependent on Tiam1 phosphorylation by aPKC, we performed an in vitro competition assay based on the experiments described in Figure 2. The Tiam1-binding region of PAR3, PAR3-4N (Supplemental Figure S5A), efficiently pulled down Tiam1-PHnCCEx, either alone or in the presence of the control competitor protein MBP (Figure 3, C and D). However, when MBP-Tiam1-N/1-WT was introduced as the competitive element, the PHnCCEx pull-down efficiency was significantly reduced. Of importance, the addition of the phosphomimetic N-terminal fragment abolished this titration effect, demonstrating that aPKC phosphorylation of Tiam1 regulates its protein–protein interactions through the PHnCCEx domain (Figure 3, C and D).

We next examined the potential regulation of Tiam1 GEF activity by the N-terminal region of Tiam1. Several previous reports
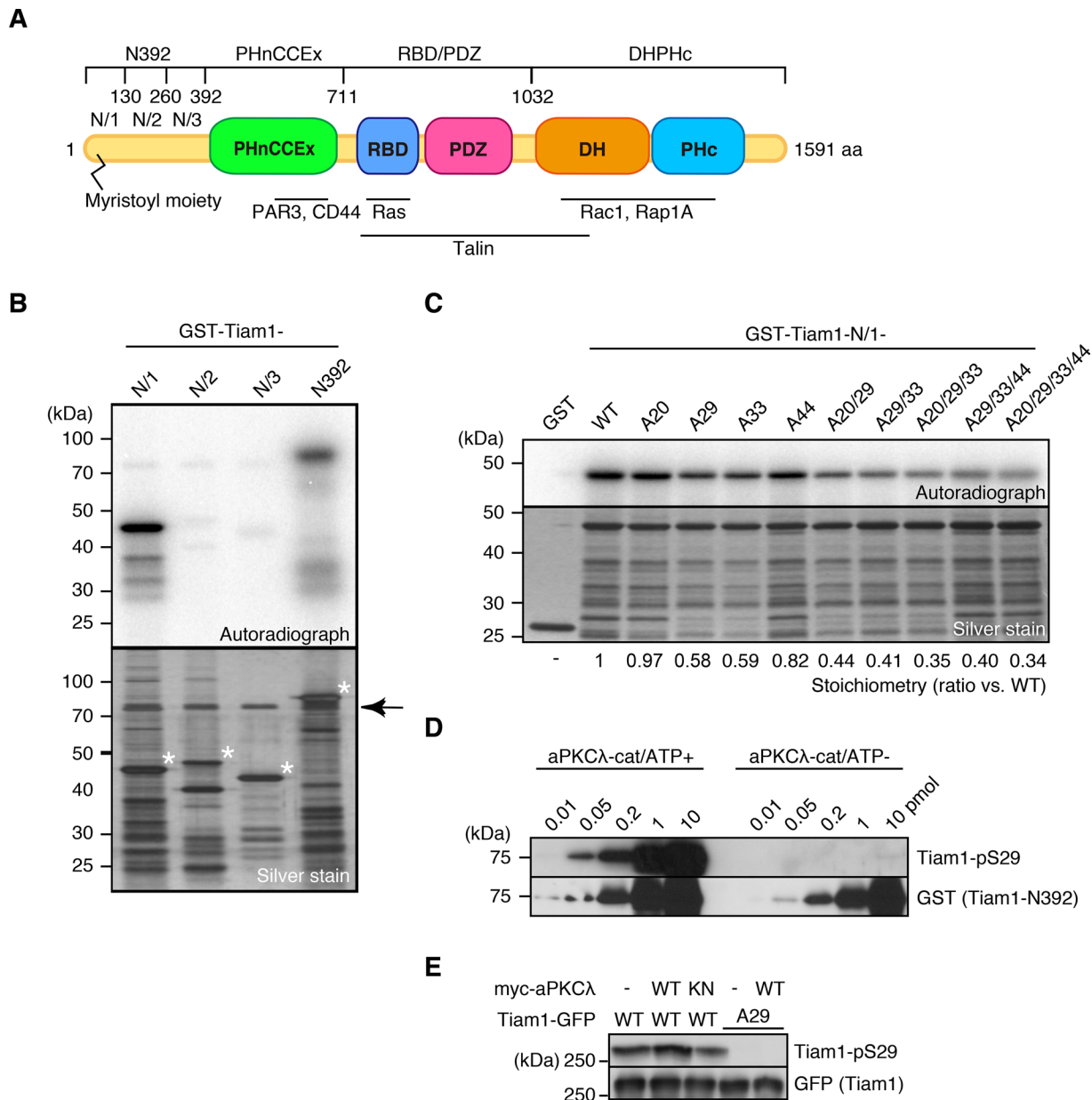
FIGURE 1: Tiam1 is phosphorylated by aPKC at serine residue 29 in vitro and in cells. (A) Schematic overview of Tiam1. The domain organization and the fragments used. The N-terminal PH domain together with the CC and Ex regions constitute a functional domain. Representative protein interactors. (B) The N-terminal-most 130 amino acids of Tiam1 are phosphorylated by aPKC in vitro. The GST-fused N-terminal Tiam1 fragments (indicated by asterisks in the silver-stained gel image) were incubated with GST-aPKCλ-cat in the presence of [γ-^{32}P]ATP, and phosphorylation was determined by autoradiography. The arrow indicates GST-aPKCλ-cat. (C) Ser-29 and Ser-33 of Tiam1 are specifically phosphorylated by aPKC in vitro. GST-Tiam1-N/1 (1–130) harboring alanine mutations of the serine and threonine residues within the N-terminal-most 50 amino acids were prepared, and an in vitro phosphorylation assay was performed as described in B. (D, E) The immunoreactivity of the phosphorylated anti-Tiam1 antibody (anti-Tiam1-pS29) is phosphorylation-site specific. The antibody was purified from a rabbit inoculated with a Tiam1 peptide phosphorylated at serine 29. (D) The anti-Tiam1-pS29 antibody specifically recognizes the in vitro–phosphorylated Tiam1 N-terminal fragment. GST-Tiam1-N392 (1–392) was incubated with GST-aPKCλ-cat in the presence or absence of [γ-^{32}P]ATP and immunoblotted with anti-Tiam1-pS29 antibody. (E) aPKCλ coexpression with Tiam1 induces an increase in Tiam1-pS29 immunoreactivity. COS-7 cells were transfected with Tiam1-HA and the indicated myc-aPKC constructs, and the lysates were immunoblotted with the indicated antibodies. Experiments shown are representative of at least three independent experiments.

showed that the binding of phospholipids, namely phosphatidylinositol 5-phosphate (PtdIns5P), to PHc can up-regulate Tiam1 GEF activity (Baumeister et al., 2003; Viaud et al., 2014). Thus we attempted to analyze the role of aPKC phosphorylation within this framework. The de novo synthesis of 5-phosphate phospholipids was suppressed by treatment of NIH-3T3 cells with an inhibitor of the phosphatidylinositol phosphate kinase, PIKfyve, which inhibits the formation of phosphatidylinositol 3,5-bisphosphate and PtdIns5P (Jefferies et al., 2008). The inhibitor treatment significantly decreased Akt-S473 phosphorylation, which requires the presence
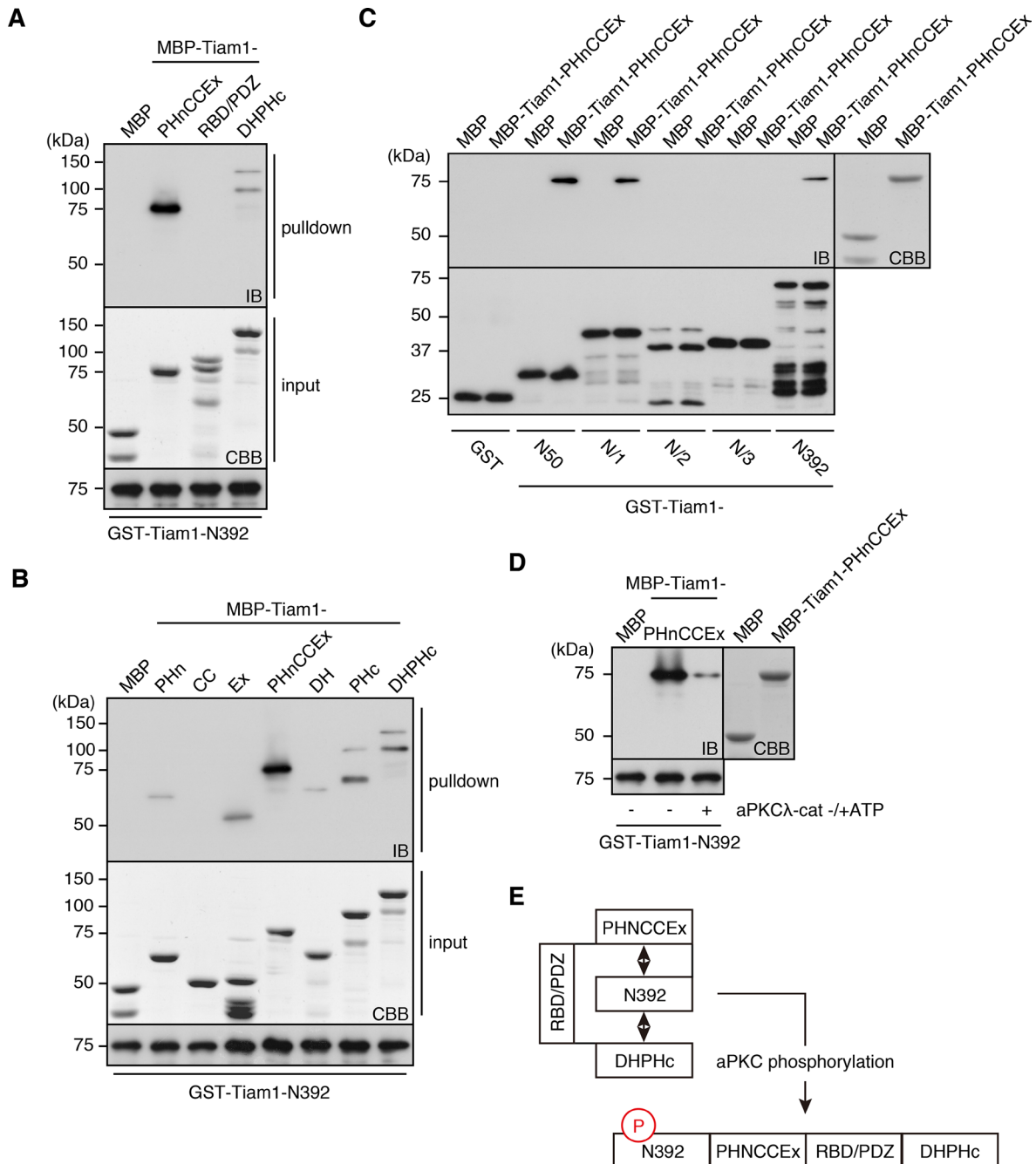
FIGURE 2: Intramolecular interactions of Tiam1 are reversibly regulated by aPKC phosphorylation. (A) The N-terminal region of Tiam1 binds intramolecularly to its PHnCCEx and DHPHc domains. GST-Tiam1-N392 was incubated with the indicated MBP-fused Tiam1 fragments (shown schematically in Figure 1A). (B) The PHn and Ex subdomains of PHnCCEx are required for binding to the N-terminal region of Tiam1. GST-Tiam1-N392 was incubated with the MBP-fused Tiam1-PHnCCEx subdomains PHn, CC, and EX. (C) The N-terminal-most 50 amino acids of Tiam1 are sufficient to bind Tiam1-PHnCCEx. The GST-fused N-terminal Tiam1 deletion fragments were incubated with MBP-Tiam1-PHnCCEx. (D) Phosphorylation of the N-terminal region of Tiam1 by aPKC abolishes its interaction with the PHnCCEx domain. GST-Tiam1-N392 was incubated with GST-aPKCλ-cat in the absence or presence of ATP and subsequently assayed against MBP-Tiam1-PHnCCEx. (E) Schematic representations of the "closed" and "open" Tiam1 conformations resulting from the aPKC-regulated intramolecular interactions. All experiments shown are representative of at least three independent experiments.

of phosphatidylinositol 3,4,5-trisphosphate, even under normal growth conditions, suggesting that the bulk 5-phosphate phospholipid level was suppressed (Supplemental Figure S2). In light of this observation, we serum starved NIH-3T3 cells expressing either the WT or the phosphomimetic DD mutant of Tiam1 overnight in the presence of a PIKfyve inhibitor. The cells were restored by incubation in normal growth medium without the PIKfyve inhibitor for 10 min before being subjected to pull down using GST-Rac1-A15, which specifically associates with active GEFs (García-Mata *et al.*, 2005). Under this condition, the pull-down efficiency of the WT
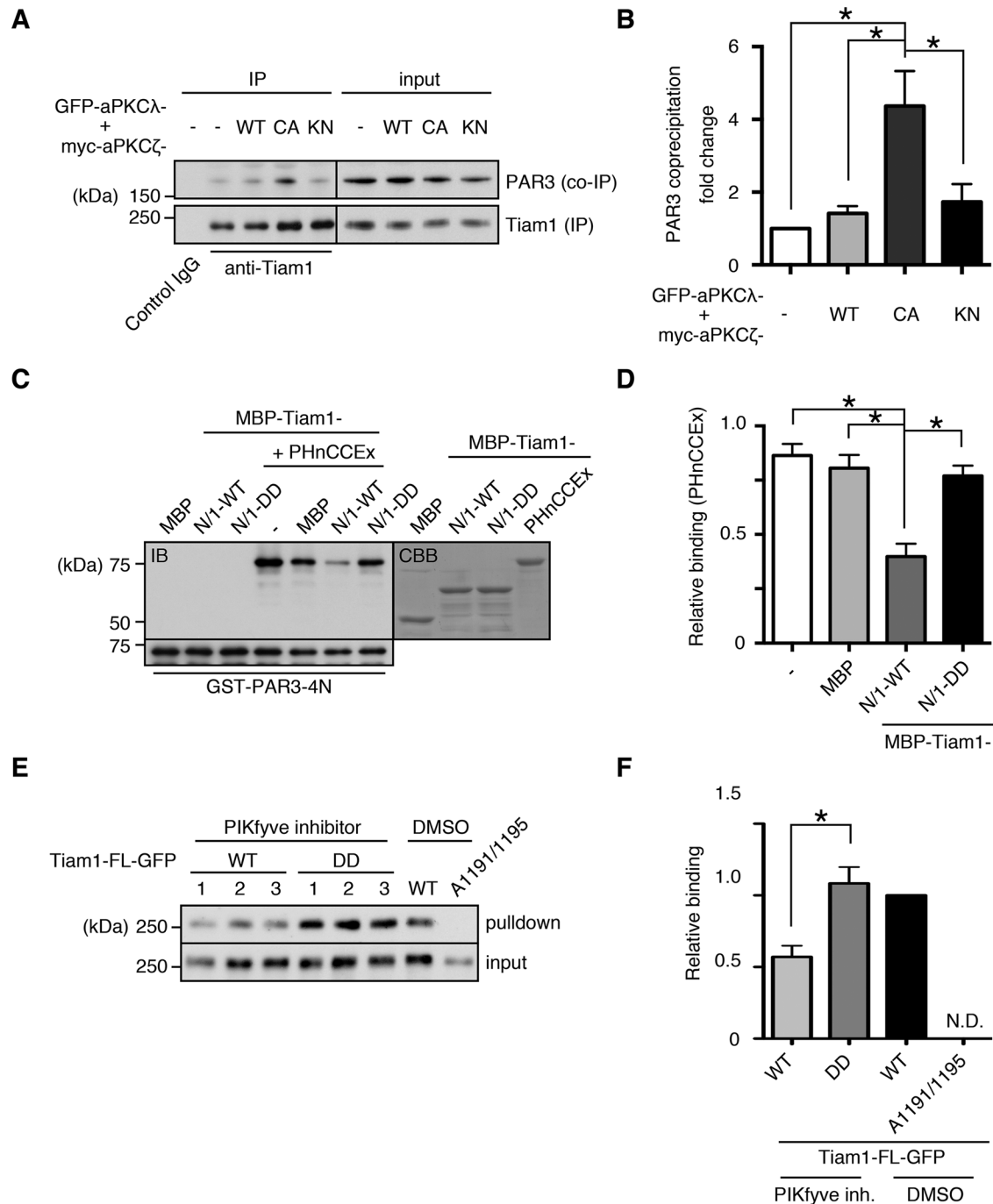
FIGURE 3: Tiam1 is functionally regulated by intramolecular interactions and aPKC phosphorylation. (A) Constitutive aPKC activation enhances the Tiam1-PAR3 interaction. Tiam1 was immunoprecipitated from NIH-3T3 lysates expressing WT, constitutively active (CA), or KN mutants of aPKCs, and the immunoprecipitates were immunoblotted with the indicated antibodies. (B) Quantification of A. PAR3 coprecipitation was normalized to Tiam1 immunoprecipitation, and the fold change relative to the vector control was plotted. (C, D) WT N-terminal region of Tiam1, but not the phosphomimetic (DD) N-terminal region of Tiam1, interferes with Tiam1 binding to PAR3. GST-PAR3-4N was incubated with MBP-Tiam1-PHnCCEx, and the interaction was titrated by a molar excess of MBP alone, MBP-Tiam1-N/1-WT, or MBP-Tiam1-N/1 in which serine residues 29 and 33 were mutated to aspartate (–DD). (C) Representative immunoblot. (D) Quantification of C. (E, F) aPKC phosphorylation of Tiam1 primes its activation. WT, the phosphomimetic mutant (DD), and the GEF activity-deficient mutant (A1191/1195) of Tiam1 were expressed in NIH-3T3 cells and subjected to pull down by GST-Rac1-A15. The lysates were immunoblotted with GFP antibody. The experimental cells were serum starved and treated with 100 nM PIKfyve inhibitor for >12 h before normal growth medium was restored for 10 min immediately before cell lysis. The control cells were cultured in dimethyl sulfoxide–supplemented normal growth medium throughout the duration of the assay. (E) Representative immunoblot. The triplicate samples are numbered. (F) Quantification of E. N.D., not detected. All experiments shown are representative of at least three independent experiments. Error bars indicate the SEM; *$p < 0.05$.
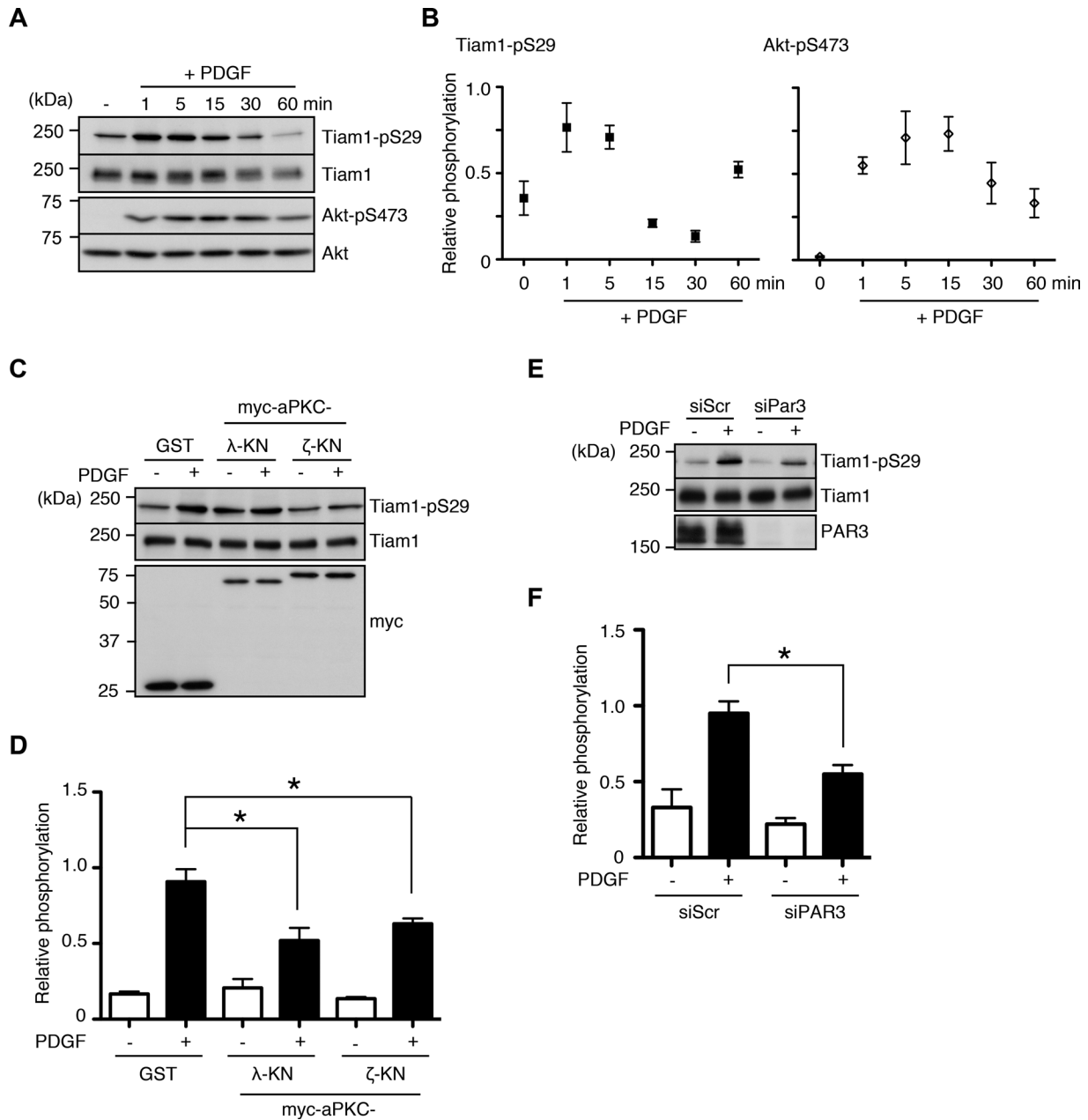
FIGURE 4: aPKC and PAR3 mediate Tiam1-S29 phosphorylation during PDGF signaling. (A, B) PDGF stimulation enhances Tiam1-S29 phosphorylation. Serum-starved NIH-3T3 cells were treated with 50 ng/ml PDGF for the indicated times, and the lysates were immunoblotted with the indicated antibodies. (C–F) aPKC activity and PAR3 are required for PDGF-induced Tiam1-S29 phosphorylation. (C, D) NIH-3T3 cells were transfected with KN mutants of either myc-aPKCλ or ζ, serum starved, and treated with PDGF for 5 min. The lysates were immunoblotted with the indicated antibodies. (E, F) PAR3 expression was knocked down by siRNA treatment in NIH-3T3 cells before PDGF stimulation, as in C and D. At least three independent experiments for each experiment shown. Error bars indicate the SEM; *$p < 0.05$.

protein was significantly reduced compared with the WT control (Figure 3, E and F). However, the phosphomimetic DD mutant was pulled down with a similar efficiency as the untreated WT control, suggesting that aPKC phosphorylation facilitates Tiam1 activation, potentially through mechanisms involving phosphoinositides.

PDGF stimulation induces Tiam1 phosphorylation by aPKC, which is mediated by PAR3

Growth factor signaling through RTKs leads to Rac1 activation, cytoskeletal remodeling, and cell polarization (reviewed in Burridge and Wennerberg, 2004). It was previously shown that PDGF stimulation

of NIH-3T3 cells induces the membrane translocation of Tiam1 and enhances its phosphorylation at threonine residues (Buchanan *et al.*, 2000). Thus we sought to study the significance of Tiam1-S29 phosphorylation in the context of PDGF signaling. When we treated serum-starved NIH-3T3 cells with PDGF, we observed rapid induction of Tiam1-S29 phosphorylation, with a peak phosphorylation time course of 1 min. This is in contrast to Akt phosphorylation, which increased more gradually (Figure 4, A and B). Tiam1-S29 phosphorylation in response to PDGF stimulation was at least partially dependent on aPKCs, since the expression of KN versions of the two isoforms reduced phosphorylation levels, whereas pharmacological

A

B

C
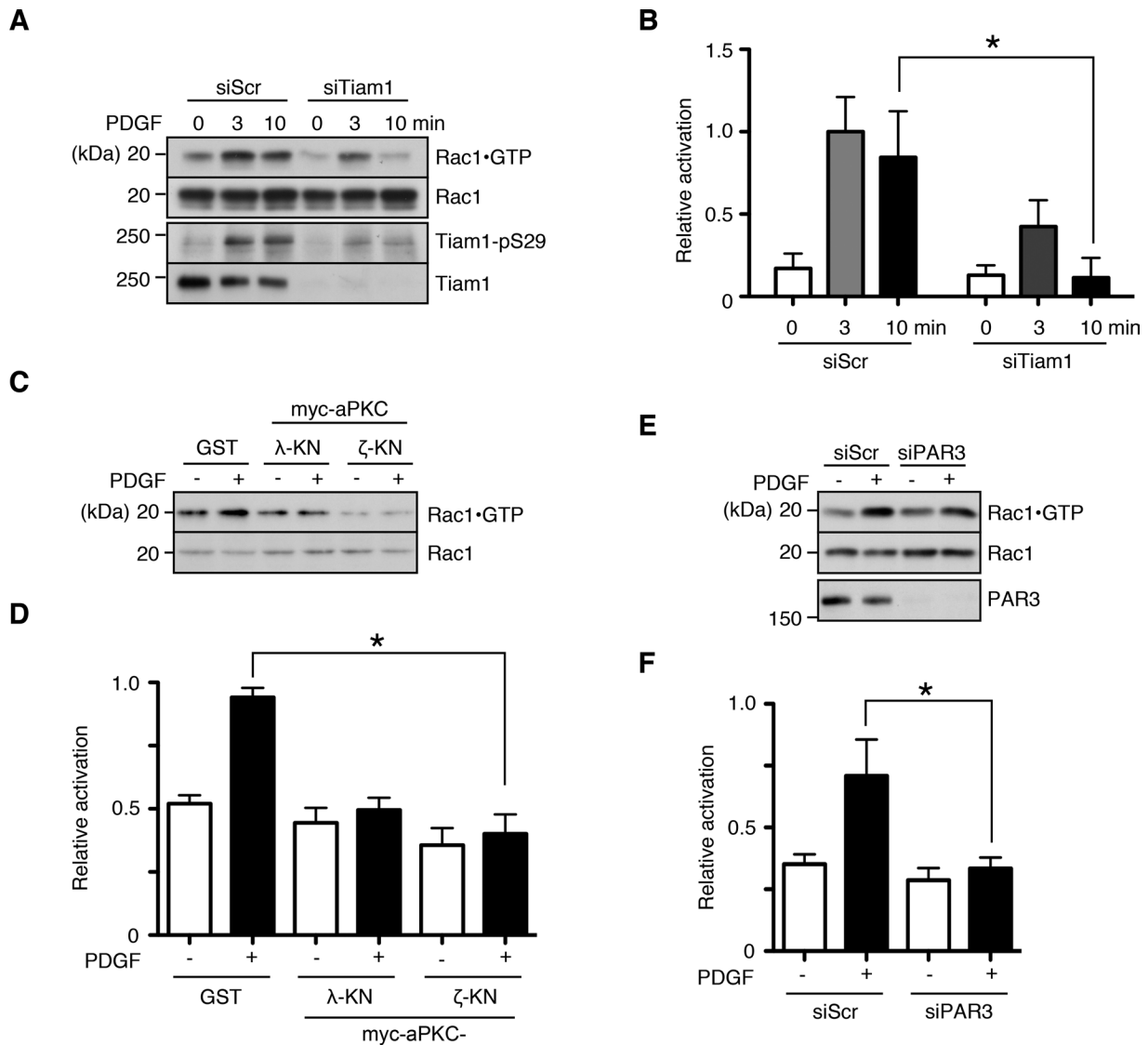

D

E

F

FIGURE 5: Tiam1, aPKC, and PAR3 are required for the acute PDGF-induced activation of Rac1. (A, B) Tiam1 is required for PDGF-induced Rac1 activation. The NIH-3T3 cells were transfected with an siRNA against Tiam1, serum starved, and stimulated with PDGF for the indicated times. Activated Rac1 was pulled down by incubating the lysates with the GST-fused CRIB region of PAK. The lysates and precipitates were immunoblotted with the indicated antibodies. (C–F) aPKC activity and PAR3 are required for the acute activation of Rac1 in response to PDGF treatment. (C, D) The NIH-3T3 cells were transfected with KN mutants of either myc-aPKCλ or ζ, serum starved, and treated with PDGF for 5 min. Activated Rac1 was detected as in A and B. (E, F) PAR3 expression was knocked down by siRNA treatment in NIH-3T3 cells before PDGF stimulation as in C and D. Activated Rac1 was detected as in A and B. At least three independent experiments for each experiment shown. Error bars indicate the SEM; *$p < 0.05$.

inhibition of the conventional PKC isoforms α and β had no effect on phosphorylation levels (Figure 4, C and D, and Supplemental Figure S3). Of interest, PAR3 was also required for full induction of Tiam1 phosphorylation (Figure 4, E and F). Because protein phosphorylation levels are regulated by the balance between the actions of kinases and phosphatases, these results suggest that PDGF stimulates Tiam1-S29 phosphorylation in vivo and that the turnover of this phosphorylation is rapid.

Tiam1 phosphorylation by aPKC is required for PDGF-induced Rac1 activation and dorsal ruffle formation

To establish whether Tiam1 is required for Rac1 activation in response to PDGF stimulation, we performed a pull-down assay based on the Cdc42/Rac interactive binding (CRIB) motif of the Rac1 effector PAK,

which enables detection of active Rac1. When Tiam1 expression was knocked down by siRNA transfection, PDGF-induced Rac1 activation was significantly reduced (Figure 5, A and B). Similar to the results in Figure 4, interfering with aPKC activity and PAR3 expression also resulted in suppressed Rac1 activation (Figure 5, C–F).

At the cellular level, growth factor–induced Rac1 activation manifests as cytoskeletal changes, such as peripheral and circular dorsal ruffles (Ridley et al., 1992; reviewed in Burridge and Wennerberg, 2004). We investigated the role of Tiam1 in the PDGF-induced remodeling of the actin cytoskeleton in NIH-3T3 fibroblasts by small interfering RNA (siRNA)–mediated knockdown. A significant proportion of control siRNA–transfected cells (>50%) formed prominent dorsal ruffles 10 min after PDGF treatment, which were largely absent when Tiam1 expression was suppressed (Figure 6A and
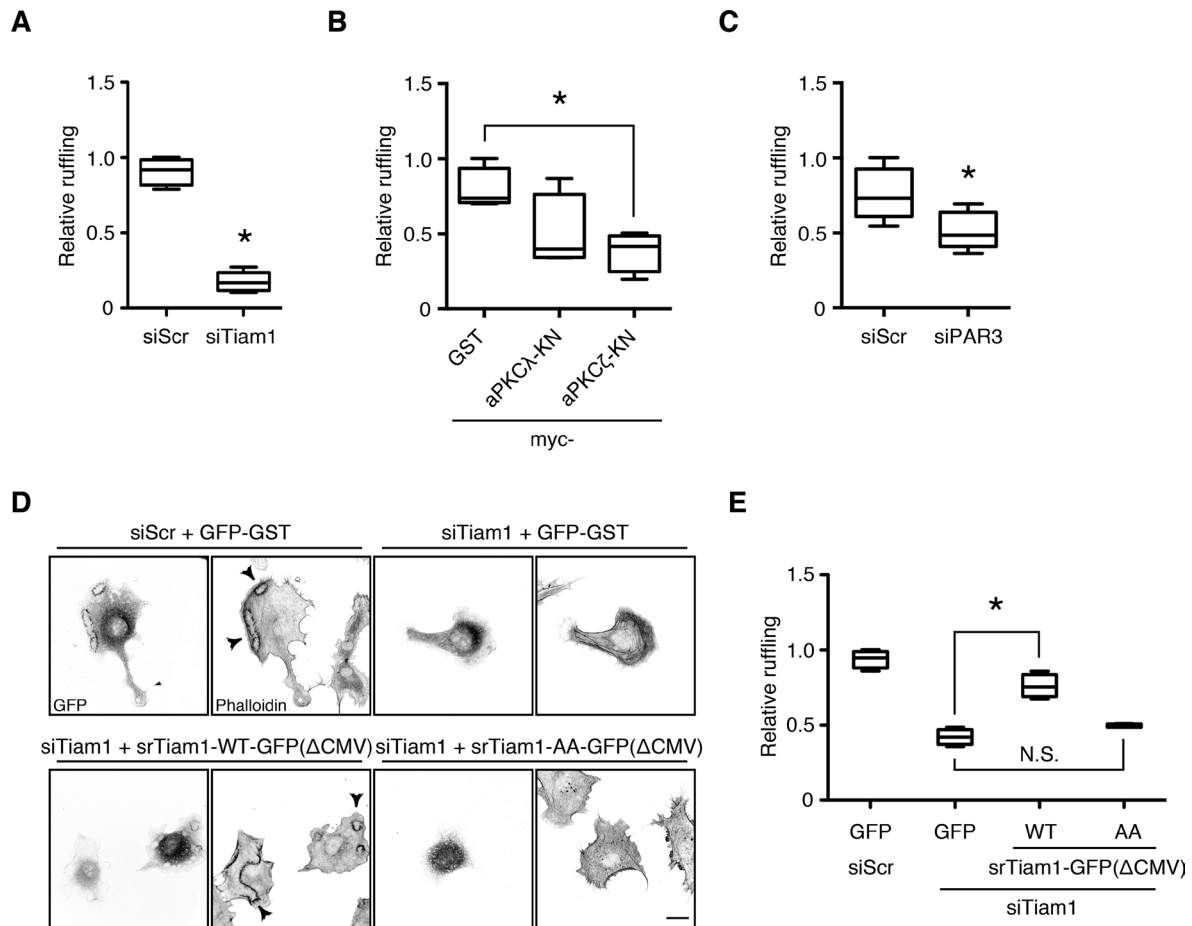
FIGURE 6: Tiam1 phosphorylation by aPKC is required for PDGF-induced dorsal ruffle formation. (A–C) Tiam1, aPKC, and PAR3 regulate dorsal ruffle formation in response to PDGF stimulation. The NIH-3T3 cells were transfected with (A) the Tiam1 siRNA, (B) myc-aPKCλ or ζ-KN, or (C) the PAR3 siRNA and seeded on poly-D-lysine–coated coverslips. The serum-starved cells were stimulated with PDGF for 7 min. Dorsal ruffles were visualized by phalloidin staining and quantitated as detailed in *Materials and Methods*. (D, E) Phosphorylation of Tiam1 at S29 and S33 is required for PDGF-induced dorsal ruffle formation. The NIH-3T3 cells were transfected with a Tiam1 siRNA and an siRNA-resistant Tiam1-GFP(ΔCMV) (see *Materials and Methods*), either WT (–WT) or that harboring the nonphosphorylatable alanine mutations of serine residues 29 and 33 (–AA). Dorsal ruffle visualization and quantification were performed as in A–C. At least three independent experiments for each experiment shown. Scale bar, 20 μm. Error bars indicate the SEM; *$p < 0.05$; N.S., no statistical significance.

Supplemental Figure S4). Of interest, Tiam1 silencing did not appear to affect the peripheral ruffle formation at later time points (Supplemental Figure S4). Similarly, attenuating aPKC activity by expressing dominant-negative aPKC constructs significantly reduced dorsal ruffle formation, as did suppressing PAR3 expression, although to a lesser degree (Figure 6, B and C).

To establish that aPKC mediated PDGF-induced dorsal ruffles specifically through Tiam1 phosphorylation, we performed a rescue experiment. The expression of WT Tiam1 in NIH-3T3 cells transfected with the Tiam1 siRNA significantly increased the rate of dorsal ruffle formation compared with the vector control (Figure 6, D and E). Of importance, the expression of the nonphosphorylatable Tiam1 mutant failed to restore dorsal ruffle formation (Figure 6, D and E). These results suggest that aPKC phosphorylation of Tiam1 specifically regulates its ability to efficiently activate Rac1 in response to PDGF stimulation and that PAR3 also mediates this process.

Tiam1, PAR3, and aPKC interact with PDGF receptor β

Receptor tyrosine kinases and their associated signaling proteins are compartmentalized in defined membrane microdomains

(reviewed in Simons and Sampaio, 2011). Therefore we examined whether Tiam1 can form a complex with the PDGF receptor. When either Tiam1 or PDGFRβ was immunoprecipitated, the opposite proteins were reciprocally coprecipitated (Figure 7A). Of note, phosphorylated Tiam1 also interacted with PDGFRβ (Figure 7B). PAR3 and aPKC were identified not only in the Tiam1 immunoprecipitate, as expected, but also in the PDGFRβ immunoprecipitate (Figure 7A).

The recovery rate of PAR3 from the PDGFRβ immunoprecipitate was consistently higher than that of Tiam1, suggesting that PAR3 functions as an escort protein linking Tiam1 to PDGFRβ (Figure 7A). To validate this interaction, we performed a pull-down assay using lysates from COS-7 cells coexpressing GST-fused cytosolic tail (CT) of PDGFRβ and myc-tagged FL PAR3 or the relevant vector controls. Myc-PAR3-FL was specifically pulled down with GST-PDGFRβ-CT (Figure 7C). We also examined whether the two proteins could directly interact in an in vitro binding assay. The C-terminal coiled-coil region of PAR3 (PAR3-4N) was specifically pulled down when the indicated PAR3 fragments were passed through columns containing GST-PDGFRβ-CT (Supplemental Figure S5, A and B).
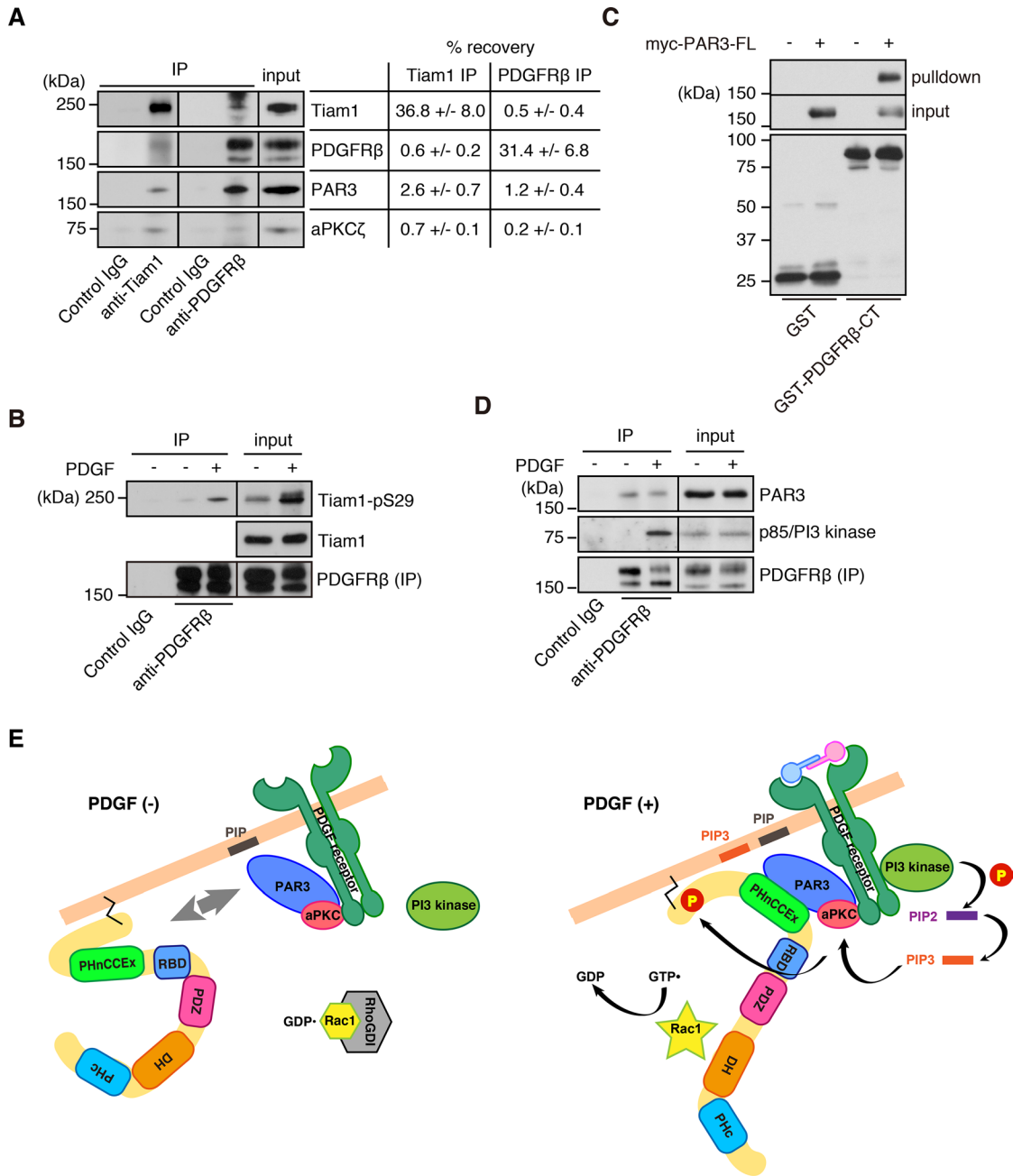
FIGURE 7: PAR3 interacts with PDGFRβ to mediate PDGF signaling to Rac1 through Tiam1. (A) Tiam1, aPKC, PAR3, and PDGFRβ form a complex. Tiam1 and PDGFRβ were immunoprecipitated from NIH-3T3 cell lysates. The immunoprecipitates were immunoblotted with the antibodies shown. The percentage recovery of each protein is indicated to the left. (B) aPKC-phosphorylated Tiam1 can form a complex with activated PDGFRβ. The NIH-3T3 cells were serum starved and stimulated with PDGF. The PDGFRβ immunoprecipitates were immunoblotted with the Tiam1-pS29 antibody. (C) PAR3 interacts with PDGFRβ. GST or GST-PDGFRβ-CT (cytoplasmic tail; aa 555–1106) and myc or myc-PAR3-FL were coexpressed in COS-7 cells. The lysates were pulled down, and the precipitates were probed for GST and myc. All experiments shown are representative of at least three independent experiments. (D) PAR3 constitutively interacts with PDGFRβ. The NIH-3T3 cells were serum starved and treated with PDGF for 5 min. The lysates were subjected to immunoprecipitation with the PDGFRβ antibody. The immunoprecipitates were immunoblotted with the indicated antibodies. (E) Proposed model for the role of Tiam1 in PDGF-induced Rac1 activation. PAR3 constitutively interacts with PDGFRβ. In the absence of PDGF stimulation, Tiam1 is not phosphorylated at S29 and is biased toward a "closed" conformation, precluding a stable interaction with PAR3. On PDGF stimulation, PI3 kinase is recruited to the activated PDGF receptor β. PI3 kinase is important for two reasons. This kinase can activate aPKC and stabilize Tiam1 at the plasma membrane through the local formation of its catalytic product phosphatidylinositol (3,4,5)-triphosphate (PIP3); it can also indirectly enhance aPKC activity through its substrate, PDK. In this way, the population of Tiam1 that is transiently bound to PAR3 is simultaneously phosphorylated by aPKC and stabilized at the membrane. Thus phosphorylated Tiam1, no longer conformationally inhibited, can form a stable complex with PAR3 at sites of PDGF receptor activation to efficiently activate Rac1 in a localized manner.

Interactions between adaptor proteins and RTKs are often activity dependent, with the receptor autophosphorylation sites acting as docking sites (reviewed in Wagner et al., 2013). We tested the effect of PDGFRβ activity on its interaction with PAR3 by immunoprecipitating PDGFRβ from serum-starved and PDGF-stimulated NIH-3T3 cells. As expected, the p85 regulatory subunit of phosphoinositide 3-kinase (PI3 kinase) coprecipitated with PDGFRβ only in stimulated cells (Figure 7D, middle). However, PAR3 was comparably coprecipitated with PDGFRβ in both serum-starved and PDGF-treated cells (Figure 7D, top). Taken together, these results suggest that PAR3 constitutively interacts with PDGFRβ to mediate Tiam1 localization.

DISCUSSION

The present work demonstrates that internal interactions are important regulators of Tiam1 function and further clarifies the functional interaction between Tiam1 and the PAR complex. The N-terminal region of Tiam1 is not organized in any known coherent domain structure, and the understanding regarding its function is limited. Tiam1 contains a consensus N-terminal myristoylation motif, suggesting that it is constitutively bound to the plasma membrane through this irreversible modification. Our fractionation analysis shows that WT Tiam1 is predominantly membrane bound, whereas the majority of myristoylation-deficient mutant is cytosolic (Supplemental Figure S6, A and B). Thus addition of the myristoyl moiety appears to be an important means of targeting Tiam1 to the plasma membrane. The N-terminal region of Tiam1 also contains tandem PEST sequences, which serve as signals for protein degradation (Rogers et al., 1986); this is one reason that this region is traditionally considered inhibitory. Recently, phosphorylation of Ser-60, immediately downstream of the PEST sequences, and 14-3-3 binding to this motif were shown to be required for Tiam1 degradation, suggesting that destabilization might indeed play a regulatory role (Woodcock et al., 2009).

Proteins fluctuate under equilibrium conditions, and the range of conformations explored by these fluctuations includes both permissive/active and inhibitory/inactive structures. Moreover, protein conformations can be stably biased by posttranslational modifications in response to external cues (reviewed in Gibbs, 2014). This has been elegantly characterized in Vav proteins, a Dbl-family GEF like Tiam1 (Aghazadeh et al., 2000; Zugaza et al., 2002; Yu et al., 2010; reviewed in Bustelo, 2014). Our binding studies show that at the extremes, Tiam1 exists in a "closed" conformation, where the N-terminal region masks other functionally significant regions within the Tiam1 protein, namely, PHnCCEx and PHc, and an "open" conformation. In addition, the bias toward the "open" conformation is conferred by phosphorylation at Ser-29 (Figure 2). These intramolecular interactions could serve an inhibitory function superseding or complementary to the previously reported destabilization effect. The interaction with the PHnCCex domain ostensibly suppresses the protein–protein interactions and concomitant localization; our immunoprecipitation and in vitro titration experiments with PAR3 clearly illustrate this effect by showing that the interaction is stabilized in the presence of a permissive signal, that is, Tiam1-Ser-29 phosphorylation (Figure 3).

Similarly, we demonstrate a modulatory role for the N-terminal-PHc interaction in regulating Tiam1 GEF activity. Viaud et al. (2014) recently showed that binding of the lipid messenger PtdIns5P to Tiam1-PHc was required for its activation. Thus our experimental conditions were aimed at elucidating whether aPKC phosphorylation of Tiam1 plays a role in its activation when controlled for access to PtdIns5P. In this context, our assay for active GEF showed that

phosphorylation by aPKC can facilitate the restoration of Tiam1 activity upon removal of the cellular environment that suppresses PtdIns5P synthesis (Figure 3). Proteins are subject to a complex array of posttranslational modifications that regulate their function at multiple levels. Taken at face value, our results suggest that Tiam1-S29 phosphorylation and the accompanying structural changes are important early steps that potentiate the activation of Tiam1 by a direct modulator, such as PtdIns5P.

Our work also expands the role of the PAR complex in RTK signaling by identifying PAR3 as a novel interacting partner of PDGFRβ and revealing its role in mediating PDGF signaling to Rac1. Our finding that PAR3 directly binds PDGFRβ is one of the first reports demonstrating PAR3 interaction with an RTK; PAR3 was recently shown to bind DDR1, an atypical RTK, whose substrate is the nonsoluble extracellular matrix protein collagen (Hidalgo-Carcedo et al., 2010), and the vascular endothelial growth factor (VEGF) receptor (Nakayama et al., 2013). The interaction with the VEGF receptor is notable because the VEGF and PDGF receptor families share a single phylogenetic origin (reviewed in Andrae et al., 2008). PAR3 contains multiple PDZ domains, and PDGFRβ harbors a PDZ-binding motif. Although we found that the C-terminal coiled-coil region of PAR3 was sufficient to bind to PDGFRβ in vitro, our present results do not preclude a PDZ domain–based mode of interaction, as proposed for PAR3 and the VEGF receptor (Nakayama et al., 2013). Additional analyses are in progress to better define the mechanisms regulating this interaction.

Tiam1 is also phosphorylated at Ser-29 by hepatocyte growth factor (HGF) stimulation in epithelial Madin–Darby canine kidney II cells (Supplemental Figure S7A) and in NIH-3T3 cells upon adhesion to the extracellular matrix protein fibronectin (Supplemental Figure S7B). The PAR complex and Tiam1 were previously implicated in HGF-dependent polarized migration (Pegtel et al., 2007) and adhesion-induced cell migration (Wang et al., 2012). Taken together, these results raise the possibility that the PAR complex and Tiam1 constitute a conserved signaling unit that functions in various signaling pathways in a cell context–dependent manner. Although it is beyond the scope of the present study, this possibility merits further investigation.

MATERIALS AND METHODS
Reagents and chemicals
The following commercial antibodies were used: anti-Tiam1 (C-16) and anti-aPKCζ (H-1; Santa Cruz Biotechnology, Santa Cruz, CA); anti-PAR3 and anti-Rac1 (EMD Millipore, Darmstadt, Germany); anti-aPKCλ and anti–transferrin receptor (BD Biosciences, San Jose, CA); anti-p85, anti-Erk1/2, anti-Erk1/2-pT202/pY204, anti-Akt, anti-Akt-pS473, and anti–α-tubulin (Cell Signaling Technology, Danvers, MA); and anti-GFP and anti-GST (Sigma-Aldrich, St. Louis, MO). Anti-Myc (9E10) and anti-HA (12CA5) antibodies were purified in-house from hybridoma. Anti-MBP rabbit polyclonal antibody was raised against recombinant MBP. Anti–Tiam1-pS29 polyclonal antibody was raised against the phosphopeptide (HTSRS(-P)LRLSH; MBL, Nagoya, Japan) and was affinity purified using the phosphopeptide. The following siRNAs from Sigma-Aldrich were used: control scramble, 5′-CAGUCGCGUUUGCGACUGG-3′; siTiam1#1, 5′-GACAUUUGGGUCCAUGAAU-3′; siTiam1#2, 5′-CCGAAAUG-GUGGAGUUUCA-3′; and siPAR3#6, 5′-GGCAUGGAGACCUUG-GAAG-3′. GST-aPKCλ-cat was expressed in Sf9 cells using a baculovirus system and purified using glutathione–Sepharose beads (Amano et al., 1999). The aPKC pseudosubstrate inhibitor and the PIKfyve inhibitor YM201636 were purchased from EMD Millipore. Other chemicals were obtained from commercial sources.

Plasmid constructs

We subcloned cDNA fragments of mouse Tiam1, mouse Tiam2/STEF, rat PAR3, mouse aPKCλ, human aPKCζ, mouse Rac1, and human PDGFRβ into pGEX (GE Healthcare Life Sciences, Marlborough, MA), pMAL (New England BioLabs, Ipswich, MA), pEGFP (Takara Bio, Otsu, Japan), pCAGGS-myc, and pMT2SM-HA. For the rescue and fractionation experiments, a modified pEGFP vector with a 5′ deletion of the cytomegalovirus promoter (ΔCMV) was prepared in the manner described by Slater *et al.* (2008) to reduce the expression levels. The cDNAs encoding Tiam1, Tiam2/STEF, PAR3, aPKCλ, aPKCζ, and Rac1 were obtained as described previously (Nishimura *et al.*, 2005; Wang *et al.*, 2012; Matsui *et al.*, 2015). The PDGFRβ cDNA was obtained from DNAFORM (Yokohama, Japan). For the rescue experiments, we used siRNA-insensitive Tiam1 mutant generated with a site-directed mutagenesis kit (Agilent Technologies, Santa Clara, CA) by introducing silent mutations within the siRNA target sequence. The Tiam1 alanine and aspartate mutations, as well as the Rac1 alanine mutation, were generated in the same way. The siRNA-insensitive PAR3 and the various fragments of PAR3, Tiam1, and Tiam2/STEF were described previously (Nishimura *et al.*, 2005; Wang *et al.*, 2012).

Cell culture and transfection

COS-7 cells were cultured in DMEM with 10% fetal bovine serum, and NIH-3T3 cells were maintained in DMEM with 10% calf serum. The COS-7 cells were transfected with Lipofectamine LTX (Thermo Fisher Scientific, Waltham, MA) according to the manufacturer's protocol, and the NIH-3T3 cells were transfected using the Neon Transfection System (Thermo Fisher Scientific) according to the manufacturer's protocol. Lipofectamine RNAiMAX (Thermo Fisher Scientific) was used for the siRNA transfections.

Protein purification

Recombinant proteins were produced in *Escherichia coli* (XL-1 Blue, BL21DE3, or RosettaDE3) and purified as described previously (Wang *et al.*, 2012). Briefly, the collected bacteria were suspended and sonicated. After ultracentrifugation for 1 h at 100,000 × *g*, the supernatants were applied to columns containing glutathione–Sepharose (GE Healthcare Life Sciences) for the GST-fusion proteins or amylose resin (New England BioLabs) for the MBP-fusion proteins. After the columns were washed, the proteins were eluted with buffer containing reduced glutathione (for GST-fused proteins) or maltose (for MBP-fused proteins) and then dialyzed against the appropriate buffer. All protein purification procedures were performed at 4°C. Preparation of the GST-Rac1-A15 affinity beads was carried out as previously described (García-Mata *et al.*, 2005).

In vitro binding assay

Purified MBP-fusion proteins (50 pmol) were incubated with affinity beads coated with GST-tagged proteins (10 pmol) in buffer A (20 mM Tris-HCl, pH 8.0, 150 mM NaCl, 1 mM EDTA, 1 mM dithiothreitol [DTT], 0.1% 3-[(3-cholamidopropyl)dimethylammonio]-1-propanesulfonate, 0.1% Triton X-100, and protease inhibitors). The beads were then washed with buffer A, and the bound proteins were eluted with buffer A containing 10 mM reduced glutathione. The eluates were subjected to SDS–PAGE, followed by immunoblot analysis using an anti-MBP antibody.

Rac1 and GEF activity assays

Rac1 activity was analyzed using GST-PAK-CRIB pull downs, as previously described (Wang *et al.*, 2012). The cells were washed with ice-cold phosphate-buffered saline (PBS) and lysed with buffer B (50 mM Tris-HCl, pH 7.5, 500 mM NaCl, 1 mM MgCl$_2$, 1 mM ethylene glycol tetraacetic acid [EGTA], 0.5% NP-40, and protease and phosphatase inhibitors) containing 20 μg of GST-PAK-CRIB per sample. After removal of the debris by centrifugation, the lysates were and incubated with glutathione–Sepharose for 30 min. The beads were washed with buffer B and dissolved in SDS sample buffer. Aliquots of the lysate and eluate were immunoblotted with an anti-Rac1 antibody to monitor the total and GTP-bound activated Rac1, respectively.

Affinity precipitation of the active GEFs was performed as previously described (García-Mata *et al.*, 2005). Cell lysates were prepared in buffer C (20 mM 4-(2-hydroxyethyl)-1-piperazineethanesulfonic acid [HEPES]–NaOH, pH 7.5, 150 mM NaCl, 5 mM MgCl$_2$, 1 mM DTT, 1% Triton X-100, and protease and phosphatase inhibitors) and incubated with 100 μg of purified GST-Rac1-A15 bound to glutathione–Sepharose overnight in the cold with end-over-end agitation. The beads were then washed with buffer C and dissolved in SDS sample buffer.

Immunoprecipitation assay

Immunoprecipitation was performed essentially as described previously (Kallin *et al.*, 2004). Cells were washed with ice-cold PBS and lysed in IP buffer (20 mM HEPES-NaOH, pH 7.4, 100 mM NaCl, 5 mM EDTA, 10% glycerol, 1% Triton X-100, and protease and phosphatase inhibitors). After removal of the debris by centrifugation, the lysates were incubated with antibodies (8 μg) overnight in the cold with end-over-end mixing. Protein A–Sepharose (GE Healthcare Life Sciences) was added to the lysates, and incubation was extended for 2 h. The beads were washed with IP buffer and dissolved in SDS sample buffer.

In vitro phosphorylation assay

The kinase reaction was conducted in 50 μl of kinase buffer (20 mM Tris-HCl, pH 7.5, 5 mM MgCl$_2$, 1 mM EGTA, and 1 mM DTT) containing 100 μM [γ-^{32}P]ATP, 0.1 μM recombinant kinase (GST-aPKCλ-cat), and 1 μM substrate (purified GST-fusion proteins). After incubation for 0.5 h at 30°C, the reaction mixtures were boiled in SDS sample buffer and subjected to SDS–PAGE and silver staining. The radiolabeled bands were visualized with an image analyzer (Typhoon FLA 9000; GE Healthcare Life Sciences).

Subcellular fractionation

Subcellular fractionation was performed essentially as described in Takano *et al.* (2010). The transfected cells were collected in fractionation buffer (20 mM HEPES-NaOH, pH 7.4, 100 mM NaCl, 2 mM MgCl$_2$, 1 mM EDTA, and protease and phosphatase inhibitors) and lysed by sonication. After centrifugation at 2500 × *g* for 5 min at 4°C, the supernatant was fractionated into soluble and particulate fractions by centrifugation at 100,000 × *g* for 1 h at 4°C.

Immunohistochemical analysis

The cells were fixed with 3.7% Formalin for 15 min, followed by permeabilization with 0.25% Triton X-100 for 5 min. After incubation with blocking buffer (1 mg/ml bovine serum albumin, PBS) for 60 min at room temperature, the cells were incubated with the indicated primary antibodies overnight at 4°C and then incubated with the indicated secondary antibodies for 1 h at room temperature. The cells were observed under a confocal laser microscope (LSM5 PASCAL; Carl Zeiss, Jena, Germany) using a 1.4 numerical aperture (NA) CFI Plan-Apochromat 63× oil immersion objective lens or under an inverted microscope (IX-71; Olympus, Tokyo, Japan) using a 0.4 NA LCPlanFI 20× lens.

For the quantitative analysis of dorsal ruffle formation, PDGF-treated cells were stained for F-actin with phalloidin. Sequential micrographs covering the entire coverslip for the relevant conditions were obtained. The dorsal ruffles were systematically extracted from the binarized images by defining them as intracellular ringed structures with a circularity index value >0.7; a circularity value of 1 corresponds to a perfect circle, where circularity = $4\pi(\text{area}/\text{perimeter}^2)$. Dorsal ruffle formation was quantified as the proportion of cells that formed dorsal ruffles within the relevant cell populations. The images were processed using plug-ins bundled with the Fiji iteration of ImageJ (Schindelin *et al.*, 2012).

Statistical analysis

Student's *t* test and analysis of variance (ANOVA) were performed after the data were confirmed to fulfill the criteria of normal distribution and equal variance. If the overall ANOVA was significant, we performed a post hoc test. Tukey's honest significant difference multiple range test was performed. Statistical analyses were performed with GraphPad Prism, version 5.0 (GraphPad Software, La Jolla, CA). $p < 0.05$ was considered to indicate statistical significance.

REFERENCES

Aghazadeh B, Lowry WE, Huang XY, Rosen MK (2000). Structural basis for relief of autoinhibition of the Dbl homology domain of proto-oncogene Vav by tyrosine phosphorylation. Cell 102, 625–633.

Amano M, Chihara K, Nakamura N, Kaneko T, Matsuura Y, Kaibuchi K (1999). The COOH terminus of Rho-kinase negatively regulates rho-kinase activity. J Biol Chem 274, 32418–32424.

Andrae J, Gallini R, Betsholtz C (2008). Role of platelet-derived growth factors in physiology and medicine. Genes Dev 22, 1276–1312.

Baumeister MA, Martinu L, Rossman KL, Sondek J, Lemmon MA, Chou MM (2003). Loss of phosphatidylinositol 3-phosphate binding by the C-terminal Tiam-1 pleckstrin homology domain prevents in vivo Rac1 activation without affecting membrane targeting. J Biol Chem 278, 11457–11464.

Bourguignon LY, Zhu H, Shao L, Chen YW (2000). CD44 interaction with tiam1 promotes Rac1 signaling and hyaluronic acid-mediated breast tumor cell migration. J Biol Chem 275, 1829–1838.

Buchanan FG, Elliot CM, Gibbs M, Exton JH (2000). Translocation of the Rac1 guanine nucleotide exchange factor Tiam1 induced by platelet-derived growth factor and lysophosphatidic acid. J Biol Chem 275, 9742–9748.

Burridge K, Wennerberg K (2004). Rho and Rac take center stage. Cell 116, 167–179.

Bustelo XR (2014). Vav family exchange factors: an integrated regulatory and functional view. Small GTPases 5, e973757.

Chiu CY, Leng S, Martin KA, Kim E, Gorman S, Duhl DM (1999). Cloning and characterization of T-cell lymphoma invasion and metastasis 2 (TIAM2), a novel guanine nucleotide exchange factor related to TIAM1. Genomics 61, 66–73.

Cook DR, Rossman KL, Der CJ (2014). Rho guanine nucleotide exchange factors: regulators of Rho GTPase activity in development and disease. Oncogene 33, 4021–403.

Duman JG, Tzeng CP, Tu Y-K, Munjal T, Schwechter B, Ho TS-Y, Tolias KF (2013). The adhesion-GPCR BAI1 regulates synaptogenesis by controlling the recruitment of the Par3/Tiam1 polarity complex to synaptic sites. J Neurosci 33, 6964–6978.

García-Mata R, Wennerberg K, Arthur WT, Noren NK, Ellerbroek SM, Burridge K (2005). Analysis of activated GAPs and GEFs in cell lysates. Methods Enzymol 406, 425–437.

Gibbs AC (2014). Elements and modulation of functional dynamics. J Med Chem 57, 7819–7837.

Habets GG, Scholtes EH, Zuydgeest D, van der Kammen RA, Stam JC, Berns A, Collard JG (1994). Identification of an invasion-inducing gene, Tiam-1, that encodes a protein with homology to GDP-GTP exchangers for Rho-like proteins. Cell 77, 537–549.

Hidalgo-Carcedo C, Hooper S, Chaudhry SI, Williamson P, Harrington K, Leitinger B, Sahai E (2010). Collective cell migration requires suppression of actomyosin at cell–cell contacts mediated by DDR1 and the cell polarity regulators Par3 and Par6. Nat Cell Biol 13, 49–58.

Iden S, Collard JG (2008). Crosstalk between small GTPases and polarity proteins in cell polarization. Nat Rev Mol Cell Biol 9, 846–859.

Jefferies HB, Cooke FT, Jat P, Boucheron C, Koizumi T, Hayakawa M, Kaizawa H, Ohishi T, Workman P, Waterfield MD, Parker PJ (2008). A selective PIKfyve inhibitor blocks PtdIns(3,5)P2 production and disrupts endomembrane transport and retroviral budding. EMBO Rep 9, 164–170.

Kallin A, Demoulin J-B, Nishida K, Hirano T, Rönnstrand L, Heldin C-H (2004). Gab1 contributes to cytoskeletal reorganization and chemotaxis in response to platelet-derived growth factor. J Biol Chem 279, 17897–17904.

Matsui T, Watanabe T, Matsuzawa K, Kakeno M, Okumura N, Sugiyama I, Itoh N, Kaibuchi K (2015). PAR3 and aPKC regulate Golgi organization through CLASP2 phosphorylation to generate cell polarity. Mol Biol Cell 26, 751–761.

Mertens AE, Roovers RC, Collard JG (2003). Regulation of Tiam1-Rac signalling. FEBS Lett 546, 11–16.

Michiels F, Habets GG, Stam JC, van der Kammen RA, Collard JG (1995). A role for Rac in Tiam1-induced membrane ruffling and invasion. Nature 375, 338–340.

Michiels F, Stam JC, Hordijk PL, van der Kammen RA, Ruuls-Van Stalle L, Feltkamp CA, Collard JG (1997). Regulated membrane localization of Tiam1, mediated by the NH2-terminal pleckstrin homology domain, is required for Rac-dependent membrane ruffling and C-Jun NH2-terminal kinase activation. J Cell Biol 137, 387–398.

Miyamoto Y, Yamauchi J, Tanoue A, Wu C, Mobley WC (2006). TrkB binds and tyrosine-phosphorylates Tiam1, leading to activation of Rac1 and induction of changes in cellular morphology. Proc Natl Acad Sci USA 103, 10444–10449.

Nakayama M, Nakayama A, van Lessen M, Yamamoto H, Hoffmann S, Drexler HCA, Itoh N, Hirose T, Breier G, Vestweber D, et al. (2013). Spatial regulation of VEGF receptor endocytosis in angiogenesis. Nat Cell Biol 15, 249–260.

Nishimura T, Yamaguchi T, Kato K, Yoshizawa M, Nabeshima Y-I, Ohno S, Hoshino M, Kaibuchi K (2005). PAR-6-PAR-3 mediates Cdc42-induced Rac activation through the Rac GEFs STEF/Tiam1. Nat Cell Biol 7, 270–277.

Pegtel DM, Ellenbroek SIJ, Mertens AEE, van der Kammen RA, de Rooij J, Collard JG (2007). The Par-Tiam1 complex controls persistent migration by stabilizing microtubule-dependent front-rear polarity. Curr Biol 17, 1623–1634.

Ridley AJ, Paterson HF, Johnston CL, Diekmann D, Hall A (1992). The small GTP-binding protein rac regulates growth factor-induced membrane ruffling. Cell 70, 401–410.

Rogers S, Wells R, Rechsteiner M (1986). Amino acid sequences common to rapidly degraded proteins: the PEST hypothesis. Science 234, 364–368.

Rossman KL, Der CJ, Sondek J (2005). GEF means go: turning on RHO GTPases with guanine nucleotide-exchange factors. Nat Rev Mol Cell Biol 6, 167–180.

Schindelin J, Arganda-Carreras I, Frise E, Kaynig V, Longair M, Pietzsch T, Preibisch S, Rueden C, Saalfeld S, Schmidt B, et al. (2012). Fiji: an open-source platform for biological-image analysis. Nat Methods 9, 676–682.

Simons K, Sampaio JL (2011). Membrane organization and lipid rafts. Cold Spring Harb Perspect Biol 3, a004697.

Slater M, Hartzell D, Hartnett J, Wheeler S, Stecha P, Karassina N (2008). Achieve the protein expression level you need with the mammalian HaloTag® 7 Flexi® vectors. Promega Notes 100, 16–18.

Stam JC, Sander EE, Michiels F, van Leeuwen FN, Kain HE, van der Kammen RA, Collard JG (1997). Targeting of Tiam1 to the plasma membrane requires the cooperative function of the N-terminal pleckstrin homology domain and an adjacent protein interaction domain. J Biol Chem 272, 28447–28454.

Suzuki A, Ohno S (2006). The PAR-aPKC system: lessons in polarity. J Cell Sci 119, 979–987.

Takano T, Tsutsumi K, Saito T, Asada A, Tomomura M, Fukuda M, Hisanaga S-I (2010). AATYK1A phosphorylation by Cdk5 regulates the recycling endosome pathway. Genes Cells 15, 783–797.

Terawaki S-I, Kitano K, Mori T, Zhai Y, Higuchi Y, Itoh N, Watanabe T, Kaibuchi K, Hakoshima T (2010). The PHCCEx domain of Tiam1/2 is a novel protein- and membrane-binding module. EMBO J 29, 236–250.

Tolias KF, Bikoff JB, Burette A, Paradis S, Harrar D, Tavazoie S, Weinberg RJ, Greenberg ME (2005). The Rac1-GEF Tiam1 couples the NMDA receptor to the activity-dependent development of dendritic arbors and spines. Neuron 45, 525–538.

Tolias KF, Bikoff JB, Kane CG, Tolias CS, Hu L, Greenberg ME (2007). The Rac1 guanine nucleotide exchange factor Tiam1 mediates EphB receptor-dependent dendritic spine development. Proc Natl Acad Sci USA 104, 7265–7270.

Viaud J, Lagarrigue F, Ramel D, Allart S, Chicanne G, Ceccato L, Courilleau D, Xuereb JM, Pertz O, Payrastre B, Gaits-Iacovoni F (2014). Phosphatidylinositol 5-phosphate regulates invasion through binding and activation of Tiam1. Nat Commun 5, 4080–4080.

Wagner MJ, Stacey MM, Liu BA, Pawson T (2013). Molecular mechanisms of SH2- and PTB-domain-containing proteins in receptor tyrosine kinase signaling. Cold Spring Harb Perspect Biol 5, a008987.

Wang S, Watanabe T, Matsuzawa K, Katsumi A, Kakeno M, Matsui T, Ye F, Sato K, Murase K, Sugiyama I, et al. (2012). Tiam1 interaction with the PAR complex promotes talin-mediated Rac1 activation during polarized cell migration. J Cell Biol 199, 331–345.

Woodcock SA, Jones RC, Edmondson RD, Malliri A (2009). A modified tandem affinity purification technique identifies that 14-3-3 proteins interact with Tiam1, an interaction which controls Tiam1 stability. J Proteome Res 8, 5629–5641.

Yu B, Martins IRS, Li P, Amarasinghe GK, Umetani J, Fernandez-Zapico ME, Billadeau DD, Machius M, Tomchick DR, Rosen MK (2010). Structural and energetic mechanisms of cooperative autoinhibition and activation of Vav1. Cell 140, 246–256.

Zhang H, Macara IG (2006). The polarity protein PAR-3 and TIAM1 cooperate in dendritic spine morphogenesis. Nat Cell Biol 8, 227–237.

Zugaza JL, López-Lago MA, Caloca MJ, Dosil M, Movilla N, Bustelo XR (2002). Structural determinants for the biological activity of Vav proteins. J Biol Chem 277, 45377–45392.